Iron encrustations on filamentous algae colonized by *Gallionella*-related bacteria in a metal-polluted freshwater stream

J. F. Mori[1], T. R. Neu[2], Shipeng Lu[1,3], M. Händel[4], K. U. Totsche[4], and K. Küsel[1,3]

[1] Institute of Ecology, Aquatic Geomicrobiology, Friedrich Schiller University Jena, Dornburger Strasse 159, 07743 Jena, Germany

[2] Department of River Ecology, Helmholtz Centre for Environmental Research – UFZ, Brueckstrasse 3A, 39114 Magdeburg, Germany

[3] German Centre for Integrative Biodiversity Research (iDiv) Halle-Jena-Leipzig, Deutscher Platz 5e, 04103 Leipzig, Germany

[4] Institute of Geosciences, Hydrogeology, Friedrich Schiller University Jena, Burgweg 11, 07749 Jena, Germany

Correspondence to: Kirsten Küsel (Kirsten.Kuesel@uni-jena.de)

Abstract

Filamentous macroscopic algae were observed in slightly acidic to circumneutral (pH 5.9~6.5) metal-rich stream water that leaked out from a former uranium-mining district (Ronneburg, Germany). These algae differ in color and morphology and were encrusted with Fe-deposits. To elucidate the potential interaction with Fe(II)-oxidizing bacteria (FeOB), we collected algal samples at three time points during summer 2013 and studied the algae-bacteria-mineral compositions via confocal laser scanning microscopy (CLSM), scanning electron microscopy (SEM), Fourier transform infrared (FTIR) spectra, and a 16S and 18S rRNA gene based bacterial and algae community analysis. Surprisingly, sequencing analysis of 18S rRNA gene regions of green and brown algae revealed high homologies with the freshwater algae *Tribonema* (99.9~100%). CLSM imaging indicates a loss of active chloroplasts in the algae cells, which may be responsible for the change in color in *Tribonema*. Fe(III)-precipitates on algal cells identified as ferrihydrite and schwertmannite by FTIR were associated with microbes and extracellular polymeric substances (EPS)-like glycoconjugates. SEM imaging revealed that while the green algae were fully encrusted with Fe-precipitates, the brown algae often exhibited discontinuous series of precipitates. This pattern was likely due to the intercalary growth of algal filaments which allowed them to avoid detrimental encrustation. 16S rRNA gene targeted studies revealed that *Gallionella*-related FeOB dominated the bacterial RNA and DNA communities (70-97% and 63-96%, respectively) suggesting their capacity to compete with the abiotic Fe-oxidation under the putative oxygen-saturated conditions that occur in association with photosynthetic algae. Quantitative PCR revealed even higher *Gallionella*-related 16S rRNA gene copy numbers on the surface of green algae compared to the brown algae. The latter harbored a higher microbial diversity, including some putative predators of algae. A loss of chloroplasts in

24   the brown algae could have led to lower photosynthetic activities and reduced EPS production

25   which is known to affect predator colonization. Collectively, our results suggest the coexistence

26   of oxygen-generating algae *Tribonema* sp. and strictly microaerophilic neutrophilic FeOB in a

27   heavy metal-rich environment.

1. Introduction

Algae are known to inhabit all freshwater ecosystems including rivers, streams, lakes and even small water volumes present in pitcher plants (Stevenson et al., 1996; Cantonati and Lowe, 2014; Gebühr et al., 2006). Macroscopic algae often bloom rapidly in rivers and in small freshwater streams, such as groundwater effluents (Stevenson et al., 1996), through germination of spores, vegetative growth and reproduction (Transeau, 1916). As primary producers, these algae provide benefits for other organisms by supplying them with organic matter and oxygen via photosynthesis and are often surrounded by associated microbes (Haack and McFeters, 1982; Geesey et al., 1978; Cole, 1982; Azam, 1998). Unicellular and multicellular algae can produce polysaccharides like extracellular polymeric substances (EPS) as a shunt for carbon produced in excess during photosynthesis (Wotton, 2004; Liu and Buskey, 2000). Due to these functions, algae likely affect the activities of co-existing microbes and play important roles in microbial ecology in streams.

Some algal species have been detected in metal-polluted streams, such as hot spring effluents (Wiegert and Mitchell, 1973) and mining-impacted sites (Reed and Gadd, 1989; Warner, 1971). These algae are known to be tolerant or resistant to high concentration of metals such as Zn, Cu, Cd, Pb, Fe, and As (Reed and Gadd, 1989; Foster, 1977, 1982) and some are capable of accumulating metals (Fisher et al., 1998; Yu et al., 1999; Greene et al., 1987) which makes them ideal candidates for bio-remediation of metal-polluted sites (Yu et al., 1999; Malik, 2004). Green algae, such as *Ulothrix*, *Microspora*, *Klebsormidium*, and *Tribonema,* occur in acid mine drainage (AMD)-impacted sites (Warner, 1971; Winterbourn et al., 2000; Das et al., 2009), sometimes forming heterogeneous streamer communities (Rowe et al., 2007). Although some of

4

50 these algae show iron ochre depositions, their interactions with Fe(II)-oxidizing bacteria are not

51 well characterized.

52 A group of prokaryotes called Fe(II)-oxidizing bacteria (FeOB) mediates the oxidation of Fe(II)

53 to Fe(III) to conserve energy for growth (Colmer and Hinkle, 1947; Hanert, 2006). Most FeOB

54 are autotrophs (Johnson and Hallberg, 2009; Kappler and Straub, 2005). Biogenic Fe(III)

55 subsequently hydrolyzes and precipitates from solution forming various Fe(III)-oxides when the

56 pH exceeds 2 (Johnson et al., 2014). Aerobic acidophilic Fe(II)-oxidizers are the main drivers of

57 Fe(II)-oxidation in acidic and iron-rich freshwater environments due to low rates of chemical

58 Fe(II)-oxidation under acidic conditions (Leduc and Ferroni, 1994; Hallberg et al., 2006; Tyson

59 et al., 2004; López-Archilla et al., 2001; Senko et al., 2008; Kozubal et al., 2012). In contrast,

60 neutrophilic FeOB, such as *Gallionella* spp., *Sideroxydans* spp., or *Leptothrix* spp., have to

61 compete with a rapid chemical Fe(II)-oxidation at circumneutral pH and thus often inhabit oxic-

62 anoxic transition zones, such as sediment-water surfaces (Emerson and Moyer, 1997; Peine et al.,

63 2000; Hedrich et al., 2011b) or the rhizosphere of wetland plants, where the plant roots leak

64 oxygen and FeOB deposit Fe-minerals (known as 'Fe-plaques') on plant root surfaces (Neubauer

65 et al., 2002; Johnsongreen and Crowder, 1991; Emerson et al., 1999). *Gallionella* spp. are

66 chemolithoautotrophs that prefer microoxic conditions (Emerson and Weiss, 2004; Lüdecke et

67 al., 2010).

68 We observed macroscopic streamer-forming algae in slightly acidic to circumneutral (pH

69 5.9~6.5), metal-rich stream water flowing out of passively flooded abandoned underground mine

70 shafts in the former Ronneburg uranium mining district in Germany. This seeping groundwater

71 creates new streams and iron-rich terraces at an adjacent drainage creek bank. The filamentous

72 algae present during the summer months differed mainly in color, but all types showed iron

73   ochre deposits. Since high abundances of *Gallionella*-related FeOB were detected in the seeping

74   water and the drainage creek in previous studies (Fabisch et al., 2013, 2015), potential

75   interactions between these neutrophilic FeOB and the streamer-forming algae communities were

76   suggested.

77   Few studies have addressed the relationship between Fe(II)-oxidation and algae. A previous

78   study reported that oxygen production by cyanobacteria appeared to control Fe(II)-oxidation in

79   iron-rich microbial mats at Chocolate Pots in Yellowstone despite co-existence of anoxygenic

80   photosynthetic FeOB (Trouwborst et al., 2007), but there was no evidence of biogenic Fe(II)-

81   oxidation by chemolithotrophic neutrophilic FeOB. Another study examining a bicarbonate

82   Fe(II)-rich spring in the Swiss Alps showed the co-existence but physical separation of

83   cyanobacteria and *Gallionellaceae* (Hegler et al., 2012). Since the presence and activity of

84   neutrophilic FeOB close to oxygen-generating photosynthetic organisms has not been

85   documented, we applied different microscopic techniques to localize the Fe-minerals and

86   microorganisms on the algal surfaces and compared the bacterial community structure of

87   different algal samples to learn more about these multi-species interactions in metal-polluted

88   environments.

89

90   **2. Materials and Methods**

91   **2.1. Field site and sampling**

92   Algal samples were taken in the outflow water in the former Ronneburg uranium-mining district

93   (Thuringia, Germany) in 2013. This district in eastern Germany was one of the largest uranium

94   mining operations in the world which produced 113,000 metric tons of uranium primarily

95   through heap-leaching with sulfuric acid between 1945 and German reunification in 1990. After

the mines were closed, the open pit was filled with waste rock from the leaching heaps to prevent

further acid mine drainage (AMD). The underground mines were flooded and treated with alkali

to buffer the water to a more neutral pH. The mine water outflow began in 2010 when the water

table rose and contaminated water from the underground mine reached the surface of

surrounding grassland. The mine water outflow flowed 20 m down a hillside into the creek (Fig.

1) where red-orange terraces enriched with the Fe-oxyhydroxides goethite and ferrihydrite

formed (Johnson et al., 2014; Fabisch et al., 2015).

We sampled algae of green and brown color in July, August and September from four different

sites beginning at the outflow water (site O) and three sites further downstream (A, B, C) which

were separated from O by some artificial impoundments; the distance between A and C was 8.8

m (Fig. 1). In July 2013, we could not reach site O because it was fenced due to construction

work. Chemical parameters of water (pH, temperature, Eh, and oxygen concentration) were

measured in situ at every sampling time, using respective electrodes and meters (Mettler Toledo;

WTW, Switzerland). In addition, water collected from each site was filtered with 0.45 µm poly

vinylidene fluoride (PVDF) and acidified with HCl or HNO_3 on site and stored at 4°C until the

measurements of metals, sulfate, and organic carbon (DOC) concentrations. Algae and sediment

samples were taken from the stream with a sterilized spatula and stored at 4°C for microscopic

analyses or at -80°C for molecular biological experiments, respectively.

2.2. Geochemical characterization of the stream

Concentration of Fe(II) in water was detected using the phenanthroline method (Tamura et al.,

1974) and total Fe was determined following the addition of ascorbic acid (0.6% final

concentration). Sulfate concentration was determined using the barium chloride method

(Tabatabai, 1974). DOC in water was measured by catalytic combustion oxidation using TOC

119 analyzer (TOC-V CPN, Shimadzu, Japan). Dissolved metals (Fe, Mn, Ni, and U) in stream water

120 were measured using inductively coupled mass spectrometry (ICP-MS; X-Series II, Quadrupol,

121 Thermo Electron, Germany). Metals which accumulated on the sediments and the algae were

122 determined by ICP-MS and ICP-optical emission spectrometry (ICP-OES, 725ES, Varian,

123 Germany) after digestion. The algae sample taken at site C in August 2013 and stored at 4°C was

124 washed with deionized water on a petri dish to remove big sediment particles, then followed by

125 drying (200°C, overnight), grinding and microwave digestion (Mars XPress, CEM, Germany)

126 using HNO_3 for ICP-MS/OES measurements. The sediment samples taken at each sampling site

127 were also dried and ground, and then 0.1-0.5 g of sediments were digested using 2 ml HNO_3, 3

128 ml HF, and 3 ml $HClO_4$ for ICP-MS/OES measurements.

129 **2.3. Observation of algae under light microscope**

130 The fresh algal samples were observed on the same day as sampling under light microscope

131 (Axioplan, Zeiss, Germany). Small pieces (~5 mm) of algal bundles were picked, placed on a

132 glass slide with small amount of stream water, and then covered with a glass coverslip.

133 Microscopic images in bright field were taken with digital camera ProgRes CS (Jenoptik,

134 Germany).

135 **2.4. CLSM imaging**

136 The algal samples collected in September were examined by confocal laser scanning microscopy

137 (CLSM) using a TCS SP5X (Leica, Germany). The upright microscope was equipped with a

138 white laser source and controlled by the software LAS AF version 2.4.1. Samples were mounted

139 in a 0.5 µm deep CoverWell[TM] (Lifetechnologies) chamber and examined with a $63\times$ NA 1.2

140 water immersion lens. Algal-associated bacteria were stained with Syto9, a nucleic acid specific

141 fluorochrome. Fluorescently labelled lectin (AAL-Alexa448, Linaris), which preferentially binds

142 to fucose linked (α-1, 6) to *N*-acetylglucosamine or to fucose linked (α-1, 3) to *N*-

143 acetyllactosamine related structures and can be applied for detection of algal cell walls

144 (Sengbusch and Müller, 1983) and the microbial EPS complex (Neu et al., 2001) was used to

145 stain and detect glycoconjugates. The recording parameters were as follows: excitation at laser

146 lines 488, 568, 633 nm; emission recorded at 483-493 (reflection), 500-550 (Syto9), 580-620

147 (possible autofluorescence), 650-720 (chlorophyll A). Optical sections were collected in the Z-

148 direction with a step of 1 µm. Images were deconvolved using the option 'classic maximum

149 likelihood estimation' from Huygens version 14.06 (SVI). Lastly, image data sets were projected

150 by Imaris version 7.7.2 (Bitplane).

151 **2.5. SEM-EDX**

152 Scanning electron microscopy (SEM) was used to study the morphology of mineral precipitates

153 on algal surfaces. Droplets of sample suspensions were placed on silicon wafers and subjected to

154 air drying. High-resolution secondary electron (SE) images and energy dispersive X-ray

155 spectroscopy (EDX) were taken with an ULTRA plus field emission scanning electron

156 microscope (Zeiss).

157 **2.6. FTIR measurement for mineral precipitates on algae**

158 Fourier transform infrared (FTIR) spectra of algae encrusted with Fe-minerals were recorded

159 using a Nicolet iS10 spectrometer (Thermo Fisher Scientific, Dreieich, Germany). Mortared

160 samples were mixed with KBr (FTIR grade, Merck, Darmstadt, Germany) at a ratio of 1:100 and

161 pressed into pellets. The pellets were studied in transmission mode in the mid-infrared range

162 between 4000 and 400 cm^{-1} for a total of 16 scans at a resolution of 4 cm^{-1}. Spectra were baseline

163 corrected by subtracting a straight line running between the two minima of each spectrum and

164 normalized by dividing each point by the spectrum's maximum.

2.7. Total nucleic acids extraction from algae-microbial communities

Total nucleic acids of algae-microbial communities were extracted from ~1.4 g wet weight of algal bundle via bead beating in $NaPO_4$ buffer (pH 8.0) with TNS solution (500 mM Tris-HCl pH 8.0, 100 mM NaCl, 10% SDS wt/vol). The supernatant was taken after centrifugation, followed by extraction with equal volumes of phenol-chloroform-isoamyl alcohol [PCI, 25:24:1 (vol:vol:vol), AppliChem] and chloroform-isoamyl alcohol [CI, 24:1 (vol:vol), AppliChem]. Nucleic acids were precipitated with two volumes of polyethylene glycol (PEG) by centrifugation at 20,000 g and 4°C for 90 min. The pellets were washed with ice-cold 70% ethanol and suspended in 50 µl elution buffer (EB, Qiagen).

2.8. 18S rRNA gene-based identification of algal species

The 18S rRNA gene region of the DNA extracted from algae-microbial communities was amplified by PCR employing the universal primer pair Euk20F/Euk1179R (Euringer and Lueders, 2008) or the *Chlorophyta*-targeting primer pair P45/P47 (Dorigo et al., 2002). The PCR reactions using both primer pairs were as follows: initial denaturing at 94°C for 5 min, 25-30 cycles of denaturing at 94°C for 30 s, annealing at 57°C for 30 s, and extension at 72°C for 90 s, and followed by final extension at 72°C for 10 min. Amplified products were purified through a spin column (NucleoSpin Gel and PCR Clean-up, Macherey-Nagel, Germany) and sequenced using Sanger technology (Macrogen Europe, Amsterdam, The Netherlands). Sequences were processed using Geneious 4.6.1 for trimming and assembling, followed by the BLAST homology search.

2.9. Quantitative PCR

Quantitative PCR was performed to elucidate the 16S rRNA gene copy numbers of *Gallionella* colonizing the algae surface using 16S rRNA gene-targeted primers specific for *Gallionella* spp.

188 (Gal122F, 5'-ATA TCG GAA CAT ATC CGG AAG T -3'; Gal384R, 5'- GGT ATG GCT GGA

189 TCA GGC -3') (Heinzel et al., 2009). Aliquots of 1.25 ng DNA were used in triplicate as the

190 template for qPCR using the Mx3000P real-time PCR system (Agilent, USA) and Maxima

191 SYBR Green qPCR Mastermix (Fermentas, Canada). Standard curves were prepared by serial

192 dilution of plasmid DNA containing the cloned 16S rRNA gene sequence of *Gallionella*

193 (accession no. JX855939). Melting curve analysis was used to confirm the specificities of the

194 qPCR products. PCR grade water and TE buffer were included as non-template controls.

195 Detailed qPCR conditions were described by Fabisch et al. (Fabisch et al., 2013).

2.10. Amplicon pyrosequencing

197 16S rRNA gene-targeted amplicon pyrosequencing was performed to reveal the population

198 structures of bacteria on the algae. To determine the bacterial community composition based on

199 RNA, cDNA samples were prepared as follows: 3.3-6.0 µg of total nucleic acids extracted from

200 algae-microbial communities were treated with DNase using TURBO DNA-*free*™ Kit (Ambion,

201 USA) to remove all DNA, and then 0.3-0.5 µg of DNase-treated RNA samples were transcribed

202 to cDNA using RETROscript® Kit (Life Technologies, CA) and stored at -20°C. The total

203 nucleic acid samples (as DNA samples) and cDNA samples were sent to the Research and

204 Testing Laboratory (Lubbock, TX, USA) for pyrosequencing of the V4-V6 region. Samples were

205 sequenced on a Roche 454 FLX system using tags, barcodes and forward primers listed in Table

206 S1. Sequence reads were processed in Mothur 1.33.0 (Schloss et al., 2009) for trimming, quality

207 checking, screening, chimera removal, and alignment based on the Silva reference alignment

208 files provided on the Mothur website (http://www.mothur.org/wiki/Silva_reference_files).

209 Dendrograms were constructed in Mothur using unweighted pair group method arithmetic

210 averages (UPGMA) based on Bray-Curtis index (Bray and Curtis, 1957) to estimate similarity

211   among bacterial DNA and RNA community compositions in each sample. Sequences originating

212   from algal chloroplasts were removed for statistical analysis of community composition. Gini-

213   Simpson index was calculated using Mothur.

214

215   **3. Results**

216   **3.1. Characterization of algae-bacterial assemblage**

217   Abundant macroscopic filamentous algae up to 10 cm length appeared at the outflow site (O)

218   (Fig. 1) and further downstream at sites A, B, and C during the summer months. Algae were

219   often covered by orange-colored minerals. The outflow water was suboxic (1.3-2.0 mg l^{-1}

220   oxygen) at site O with a slightly acidic pH of 5.9, however, water became more oxygenated (6.2-

221   6.9 mg l^{-1} oxygen) and had a higher pH (6.4-6.5) further downstream (Fig. 2). The increase in

222   oxygen could be caused by both turbulent mixing with air and photosynthetic activities of the

223   algae and increase of pH likely resulted from a combination of CO_2 outgassing from the initial

224   anoxic outflow water and draw down of CO_2 via algal growth. The water temperature was

225   approximately 14-17°C at site O during sampling. Dissolved iron in the water was primarily in

226   the form of Fe(II) with maximum concentrations of 3.3 mM and decreased in concentration (to

227   2.1 mM) as the water moved downstream towards sites A, B, and C. The other parameters

228   measured did not indicate distinct differences between the sites O, A, B, and C (Eh, 140-180

229   mV; conductivity, 4.8-4.9 ms cm^{-1}; DOC, 3.0-4.5 mg l^{-1}; sulfate concentration, 30-35 mM; Fig.

230   2). The stream water was also enriched with other metals including Mn, Ni, Zn and U.

231   In July 2013, we sampled green algae from sites A and B (algae at site O could not be reached),

232   and brown algae from site C. During a subsequent sampling during August 2013, the algae

233   collected from site B changed in color from green to brown, while algae samples collected from

234 sites O and A still appeared green. By September 2013, most algae had disappeared; only small

235 amounts of green algae were left at site O and some brown algae at site A (Table 1). Sequencing

236 analysis of 18S rRNA gene regions amplified from DNA extracts of green and brown algae

237 showed that all algae had high homologies with *Tribonema* spp. (*T. viride*, *T. minus*, *T.*

238 *ulotrichoides*, 99.9~100%; Table S2), a genus of freshwater algae belonging to the class of

239 *Xanthophyceae*.

240 Microscopic observations revealed unbranched filamentous algae with a single cell length of 30-

241 50 µm and a cell diameter of 8-10 µm (Fig. 3C, D, 4A, B, C). Green algae cells yielded 10-15

242 visible chloroplasts which exhibited strong autofluorescence, whereas brown algae cells

243 contained only 5-7 countable chloroplasts and displayed weaker autofluorescence. The brown

244 algae often showed green autofluorescence under UV-light exposure (data not shown), which

245 likely resulted from flavin-like molecules or luciferin compounds (Tang and Dobbs, 2007). This

246 green autoflouresence was not detected in the green algae, likely due to stronger signals from

247 chloroplasts. According to the cell morphology and number of chloroplasts per cell, the green

248 and brown algae display a high degree of similarity to *T. viride* comparing to *T. minus* and *T.*

249 *ulotrichoides* (Akiyama et al., 1977; Gudleifsson, 1984; H. Wang et al., 2014).

250 Minerals adhered to and were distributed in a regular discontinuous pattern on the surface of the

251 brown algae. In contrast, the surface of the green algae was encrusted with minerals in irregular

252 shape, size and location (Fig. 3C, D, 4A, B). CLSM images using Syto9 stain showed minerals

253 adhered to the surface of both brown and green algae that were colonized by microorganisms

254 (Fig. 4A, B). These microbial cells primarily colonized the minerals attached to the algae

255 surfaces, while a smaller proportion of microbial cells were adhered directly to the algae bodies.

256 Neither stalks of *Gallionella* nor other characteristic extracellular structures of FeOB were found

257 on the algae. CLSM images with lectin staining showed the cell sections in algal filaments were

258 distributed between regularly located Fe-minerals. In addition, algal or bacterial EPS-like

259 glycoconjugates were likely associated with the minerals (Fig. 4C), whereas the amount of EPS

260 could not be quantified or compared between the green and brown algae.

261 **3.2. Component analysis of mineral precipitates on the algae**

262 Secondary electron (SE) images with EDX analyses showed sulfur-containing Fe-oxides almost

263 completely covered the surface of the green algae (Fig. 5A, 6A), whereas some areas on the

264 surface of the brown algae were not encrusted (Fig. 5B, 6B). The non-encrusted parts of the

265 brown algae primarily displayed background signal (i.e. Si signal of the sample holder). Weak

266 signals of C, Mg, Ca and P were also detected by EDX. The elemental composition of Fe-oxides

267 not associated with algae was almost identical to those of the encrusted algae, suggesting mineral

268 composition was not affected by biological activity.

269 FTIR spectra exhibited signals of ferrihydrite and schwertmannite (Fig. 6C). Their presence was

270 also confirmed by high resolution SE images. Spherical aggregates with nano-needles on the

271 surface edges are defining characteristics for schwertmannite (Fig. S1), while aggregates with no

272 single crystallites are often composed of ferrihydrite (Carlson et al., 2002). The FTIR spectra of

273 minerals on the green algae also showed weak signals of Si-O bonding at 1030 cm^{-1}, which

274 might be due to residual clay minerals.

275 Total extractions of the brown algae collected at site C revealed that in addition to Fe, Mn, Ni,

276 Zn and U accumulated on the algae surface similarly to the underlying sediments at site C (Fig.

277 S2); Fe and U even showed higher concentrations on the surface of the algae in comparison to

278 the sediment (540 mg of Fe and 910 µg of U in 1 gdw algae and 390-660 mg of Fe and 90-750

279 µg of U in 1 gdw sediment).

3.3. Elucidating the bacterial community structure associated with algae

Quantitative PCR detected high gene copy numbers (per gram wet weight algae) for *Gallionella*-related 16S rRNA with slightly higher numbers for the green algae $(1.72 \times 10^9 – 7.08 \times 10^9)$ compared to brown algae (Table 1). Similarly, 16S rRNA gene-targeted amplicon pyrosequencing revealed that members of the *Gallionellaceae* were the dominant bacterial group within these algae-microbial communities when comparing both DNA and RNA samples from the green and brown algae collected at all four different sites and all time points (Fig. 7, Table S3). The relative percentage of *Gallionellaceae* was highest in RNA and DNA extracts of the green algae with 89.4-96.5% and 79.5-96.4%, respectively, of the total number of sequence reads compared to 70.4-82.9% and 62.7-81.0% in RNA and DNA extracts of the brown algae. Algal samples collected from sites O, A, B, and C during September showed the lowest fraction of *Gallionellaceae*. The *Gallionellaceae* group comprised of 2 OTUs related to the FeOB *Gallionella capsiferriformans* ES-2 (CP002159) and *Sideroxydans lithotrophicus* ES-1 (CP001965) (Table S3). The relative fraction of OTU-1-related FeOB was highest at site O, whereas OTU-2-related FeOB was more abundant downstream at sites A, B, and C. The dendrograms for each DNA and RNA community also showed that the bacterial community structures in site O were separated from those in other sites (Fig. 7). Other bacterial groups detected with less than 10% relative abundance were '*Candidatus* Odyssella' (*Alphaproteobacteria*), *Actinomycetales* (*Actinobacteria*), *Desulfobulbaceae*, and *Geobacteraceae* (*Deltaproteobacteria*). Triplicate extractions of DNA and RNA from the brown algae collected at site C in August showed little variation between bacterial community structures (Fig. 7), which allows for the identification of a representative algae surface-associated microbial community in this metal-contaminated site. The brown algae were colonized by a

303   higher diversity of bacterial groups than the green algae, showing higher average Gini-Simpson

304   index values (0.862 in RNA and 0.884 in DNA) than those of the green algae (0.641 in RNA and

305   0.645 in DNA). Interestingly, some of the sequences detected from the microorganisms adhered

306   to the brown algae surface were identified as putative predators of algae, such as '*Candidatus*

307   Odyssella' (intracellular parasite of Acanthamoeba, up to 8.1% and 6.0% of OTUs in RNA and

308   DNA extracts) and *Cystobacteraceae* (*Myxobacteria*, 2.0% and 0.2% in RNA and DNA extracts).

309

4. Discussion

311   Members of the genus *Tribonema* are known as common freshwater algae (Machova et al., 2008;

312   H. Wang et al., 2014). *Tribonema* species have been detected in other metal-rich and acidic

313   freshwater environments such as acidic brown water streams (pH <4) in New Zealand (Collier

314   and Winterbourn, 1990), acidic coal mine drainage-contaminated sites (pH 2.6-6.0)

315   (Winterbourn et al., 2000), as well as acidic rivers (pH 2.7-4.0) with iron-rich ochreous deposits

316   of schwertmannite-like Fe-minerals on algal surfaces (Courtin-Nomade et al., 2005), suggesting

317   their tolerance to high concentrations of metals and low pH. In this study, *T. viride* colonized

318   metal-rich (Fe, Mn, Ni, Zn and U) and less acidic (pH 5.9 to 6.5) mine-water outflow which

319   showed variation in geochemistry over time and along the flow paths from site O to C. The algae

320   ostensibly changed its color from green to brown and disappeared completely from sites B and C

321   at the end of the summer. The change in algae color occurred simultaneously with the loss of

322   active chloroplasts per cell, as observed via CLSM imaging. These results correspond with lower

323   numbers of sequences originating from chloroplasts based on sequences analysis. The

324   encrustation with Fe-minerals presumably inhibits algal photosynthetic activities and may be an

325   underlying cause for the disappearance of *Tribonema* at the end of the summer when light

326 intensity diminished. The observed water temperatures (14-17°C) may have also contributed to

327 the decline in algae numbers, since optimal growth temperatures of two genera of *Tribonema* are

328 higher (*T. fonticolum*, 19-27°C; *T. monochloron*, 15.5-23.5°C) (Machova et al., 2008), however,

329 *T. viride* has been detected in lake water with low temperature (0-5.6°C) (Vinocur and Izaguirre,

330 1994).

331 Deposition of Fe-minerals and colonization of "iron bacteria" on *Tribonema* was reported more

332 than 70 years ago (Chapman, 1941), but identification of the deposited minerals, the FeOB, and

333 their interaction with the alga has not been characterized in detail. A symbiotic relationship has

334 been suggested in which microbes living on the surface of *Tribonema* form ferric carbonate,

335 which controls water pH and acts as local buffer for the algae. We could not detect ferric

336 carbonates on *Tribonema,* however, poorly crystalline iron minerals ferrihydrite and

337 schwertmannite that are also present in the underlying sediments in addition to goethite were

338 detected (Johnson et al., 2014). These iron minerals have a high reactive surface area for

339 metal(loid) uptake, and particularly As and Zn appear to be associated with these minerals in the

340 sediments (Johnson et al., 2014). Brown algae showed similar metal(loid) uptake to the

341 sediments collected at the outflow downstream to site C with even higher concentrations for Fe

342 and U suggesting a high affinity of *Tribonema* for these compounds. Thus, these iron coatings

343 could also act as buffers to help prevent the plant from taking up these heavy metals, similar the

344 mechanism suggested to aid in protection from root plaque (Tripathi et al., 2014 and references

345 therein). However, since there was no pristine system without metal load around our study site,

346 we could not assess the effects of heavy metals on development of the algae-bacteria-mineral

347 communities.

348 Our microscopic investigation did not reveal a preferential colonization of microbes on the algal

349 surface but on the minerals. According to both pyrosequencing and qPCR results,

350 microaerophilic *Gallionella*-related FeOB were the dominant colonizers on *Tribonema* which

351 might be due to the presence of large populations of *Gallionella* sp. (29-58% of the total

352 bacterial community) in the outflow water reaching cell numbers of 10^5 to 10^6 cells per mL water

353 (Fabisch et al., 2015). These bacteria seem to be able to cope with the high levels of oxygen

354 produced during photosynthesis, but these oxygen concentrations may be lower within the EPS

355 matrix and ochre deposits. *G.capsiferriformans*-related FeOB predominated at the outflow site

356 whereas *S. lithotrophicus*-related FeOB dominated algae further downstream which can be

357 explained by differences in the water geochemistry such as pH or heavy metal concentrations.

358 Based on genome information, *G. capsiferriformans* ES-2 should be more resistant to heavy

359 metals than *S. lithotrophicus* ES-1 (Emerson et al., 2013) and thus should dominate the outflow

360 site which showed the highest metal loads in the water. Unfortunately, we could not link the

361 dominance of these species with the heavy metals precipitated on the algae due to shortage of the

362 present sample amount for ICP-MS/OES.

363 16S rRNA gene copy numbers of *Gallionella* on the algae surfaces (Table 1) were much higher

364 than numbers found in the sediments of the stream (3.1 x 10^8 copies per gram wet weight

365 sediment) (Fabisch et al., 2015). The high relative RNA-derived fraction of *Gallionellaceae*

366 suggested not only passive or active colonization of the algal surface but also participation in Fe-

367 oxidation followed by ferrihydrite and schwertmannite formation. *Gallionella*-related FeOB

368 appeared to be more abundant and active on the green algae, which indicates higher Fe-oxidizing

369 activity on the surface of green algae. The surface of photosynthetic algae is presumable a highly

370 oxygen-saturated environment, and the occurrence of neutrophilic microaerophilic FeOB under

such conditions has not been reported before to the best of our knowledge. However, it is possible that at night the oxygen level go to a much lower level allowing an opportunity for FeOB to grow under low oxygen. In water treatment systems and dewatering wells in open cast mines, *Gallionella* have been also reported to grow at surprisingly high oxygen concentrations at the low temperature of 13˚C or even higher which slows down abiotic Fe(II)-oxidation (de Vet et al., 2011; J. Wang et al., 2014).

In an Fe(II)-rich and oxygenated environment, bacteria potentially face the problem of highly reactive oxygen species due to the reaction of hydrogen peroxide with Fe(II) (Imlay, 2008). Both *G. capsiferriformans* ES-2 and *S. lithotrophicus* ES-1 were reported to encode enzymes that presumably act as catalase or peroxidase to prevent production of reactive oxygen species (Emerson et al., 2013). Most bacteria associated with the Fe-minerals on algae surfaces were also localized to areas where EPS-like glycoconjugates were detected. EPS forms a suitable microenvironment for microbial Fe-oxidation due to its ability to bind dissolved Fe(II) resulting from the negatively charged EPS matrix. This activity leads to the inhibition of chemical Fe-oxidation by lowering the availability of Fe(II) (Neubauer et al., 2002; Jiao et al., 2010; Roth et al., 2000). In addition, the EPS can prevent bacterial cells from being encrusted with insoluble Fe(III)-oxides (Neubauer et al., 2002; Hedrich et al., 2011a; Schädler et al., 2009). Unfortunately, with the methods used, we could not determine if the EPS-like matrix on the algae was produced by the alga or by bacteria. *Tribonema* is known to produce EPS mainly composed of glucans and xylans (Cleare and Percival, 1972), however, based on genome sequencing both *G. capsiferriformas* ES-2 and *S. lithotrophicus* ES-1 are predicted to also produce EPS (Emerson et al., 2013). In an effort to prevent encrustation, other *Gallionella* species form long stalks which are mainly composed of polysaccharides and long-chain saturated aliphatic compounds during

394 Fe(II)-oxidation with the purpose of deposition of Fe-oxides apart from the cells (Chan et al.,

395 2011; Suzuki et al., 2011; Fabisch et al., 2015; Picard et al., 2015). Stalk-forming *Gallionella*

396 have been isolated in sediment environments, but not on the surface of algae, thus implicating an

397 important role of EPS in microbial Fe-oxidation by the algae-associated bacteria. Our results

398 cannot exclude the possibility that FeOB utilize algal EPS as organic carbon source, whereas *G.*

399 *capsiferriformans* and *S. lithotrophicus* were reported to be unable to grow heterotrophically

400 (Emerson et al., 2013). The variations in color of the *Tribonema* species were accompanied with

401 a variation in encrustation patterns. The green *Tribonema* was fully encrusted whereas the brown

402 *Tribonema* showed an irregular encrustation pattern. Although *Tribonema* appears to be adapted

403 to high metal loads, excess encrustations with Fe-minerals should be detrimental due to

404 inhibition of photosynthesis and decreased access to nutrients. The lower number of chloroplast

405 pointed to decreased photosynthetic activity of the brown *Tribonema*. The discontinuous

406 encrustation might be caused by intercalary growth of the filamentous algae, which occurs by

407 generating H-shaped parts in the middle of each cell (Smith, 1938). Intercalary growth was

408 confirmed by CLSM images with lectin staining which showed algal cell sections alternating

409 with Fe-minerals. The new cell sections were thin with only a few chloroplasts suggesting that

410 energy was used primarily for elongation. Thus, intercalary growth could be interpreted as a

411 defense strategy during later stages of encrustation when photosynthetic activity diminishes due

412 to surface coverage by Fe-precipitates and to provide the algae with new uncovered cell surfaces.

413 Production of EPS as a shunt mechanism should decline if less carbon is fixed during

414 photosynthesis (Wotton, 2004) which provides a potential link between EPS production and

415 *Gallionella* colonization. Brown algae contained fewer chloroplasts, suggesting reduced

416 photosynthetic activity and EPS production which might be linked to a decrease in *Gallionella*

417　cell number and Fe(II) oxidation on the algae surface. This study showed higher microbial

418　diversity on the surface of brown *Tribonema* when lower numbers of *Gallionella* were detected.

419　Some putative predators of algae, such as '*Candidatus* Odyssella' and *Cystobacteraceae* were

420　also identified on the surface of the brown *Tribonema*. These predators colonize algae in order to

421　consume material released upon cell lysis as a natural senescence process or under stress

422　conditions (Levy et al., 2009). Algal EPS has been shown to function as a cell defense

423　mechanism to protect cells from colonization of predators or pathogens (Steinberg et al., 1997),

424　thus a reduced rate of EPS formation may lead to predator colonization.

425

426　**5. Summary and Conclusion**

427　Filamentous algae (*Tribonema* sp.) were observed in the metal-contaminated groundwater

428　outflow in the former Ronneburg uranium mining district, suggesting the algae has a tolerance to

429　high metal concentrations and metal deposits. Cells of green algae were fully encrusted with Fe-

430　oxides. The Fe-precipitates on the algae surfaces were predominantly colonized by *Gallionella*-

431　related FeOB. *Gallionella*-related FeOB were abundant in the stream water and these bacteria

432　appeared to be actively involved in Fe(II) oxidation. Thus, both sunlight and Fe(II) served as

433　energy sources for primary producers in this slightly acidic stream promoting complex microbial

434　interactions in the ochre deposits on the algal cells. EPS-like polymeric matrices, likely produced

435　as a shunt for carbon during photosynthesis, provided a suitable microenvironment for the

436　microaerophilic FeOB due to its high affinity for metal(loid)s and reduced oxygen diffusion.

437　However, excess deposition of Fe-oxides appeared to be detrimental to photosynthetic activities

438　forcing intercalary elongation of the filaments. This defense response caused discontinuous

439　deposition patterns of Fe-oxides as observed on the brown colored algae which showed lower

440 number of chloroplasts. The reduced EPS production could have favored growth of algal

441 predators on the brown algae and together with ochre deposition contributed to algal decline.

Author contribution

J. F. Mori and K. Küsel designed and J. F. Mori performed the experiments. T. R. Neu conducted CLSM imaging analysis. S. Lu carried out sampling and microscopic analysis with J. F. Mori. M. Händel and K. U. Totsche performed SEM-EDX and FTIR analysis. J. F. Mori prepared the manuscript with contributions from all co-authors.

Reference

Akiyama, M., Ioriya, T., Imahori, K., Kasaki, H., Kumamoto, S., Kobayashi, H., Takahashi, E., Tsumura, K., Hirano, M., and Hirose, H.: Illustrations of the Japanese Fresh-Water Algae, Uchidarokakuho Publishing Company, Limited, 1977.

Azam, F.: Microbial control of oceanic carbon flux: the plot thickens, Science, 280, 694-695, 1998.

Bray, J. R., and Curtis, J. T.: An ordination of the upland forest communities of southern Wisconsin, Ecol. Monogr., 27, 325-349, 1957.

Cantonati, M., and Lowe, R. L.: Lake benthic algae: toward an understanding of their ecology, Freshwater, 33, 475-486, 2014.

Carlson, L., Bigham, J. M., Schwertmann, U., Kyek, A., and Wagner, F.: Scavenging of As from acid mine drainage by schwertmannite and ferrihydrite: a comparison with synthetic analogues, Environ. Sci. Technol., 36, 1712-1719, doi:10.1021/es0110271, 2002.

Chan, C. S., Fakra, S. C., Emerson, D., Fleming, E. J., and Edwards, K. J.: Lithotrophic iron-oxidizing bacteria produce organic stalks to control mineral growth: implications for biosignature formation, ISME J., 5, 717-727, doi:10.1038/ismej.2010.173, 2011.

Chapman, V. J.: An introduction to the study of Algae, Cambrige University Press, 387, 1941.

Cleare, M., and Percival, E.: Carbohydrates of the fresh water alga *Tribonema aequale.* I. Low molecular weight and polysaccharides, Brit. Phycol. J., 7, 185-193, doi:10.1080/00071617200650201, 1972.

Cole, J. J.: Interactions between bacteria and algae in aquatic ecosystems, Annu. Rev. Ecol. Syst., 13, 291-314, 1982.

480 Collier, K., and Winterbourn, M.: Structure of epilithon in some acidic and circumneutral

481   streams in South Westland, New Zealand, New Zealand Natural Sciences, 17, 1-11, 1990.

482 Colmer, A. R., and Hinkle, M.: The role of microorganisms in acid mine drainage: a preliminary

483   report, Science, 106, 253-256, 1947.

484 Courtin-Nomade, A., Grosbois, C., Bril, H., and Roussel, C.: Spatial variability of arsenic in

485   some iron-rich deposits generated by acid mine drainage, Appl. Geochem., 20, 383-396,

486   doi:10.1016/j.apgeochem.2004.08.002, 2005.

487 Das, B. K., Roy, A., Koschorreck, M., Mandal, S. M., Wendt-Potthoff, K., and Bhattacharya, J.:

488   Occurrence and role of algae and fungi in acid mine drainage environment with special

489   reference to metals and sulfate immobilization, Water Res., 43, 883-894,

490   doi:10.1016/j.watres.2008.11.046, 2009.

491 de Vet, W. W. J. M., Dinkla, I. J. T., Rietveld, L. C., and van Loosdrecht, M. C. M.: Biological

492   iron oxidation by *Gallionella* spp. in drinking water production under fully aerated

493   conditions, Water Res., 45:17, 5389-5398, doi:10.1016/j.watres.2011.07.028, 2011.

494 Dorigo, U., Berard, A., and Humbert, J. F.: Comparison of eukaryotic phytobenthic community

495   composition in a polluted river by partial 18S rRNA gene cloning and sequencing, Microb.

496   Ecol., 44, 372-380, doi:10.1007/s00248-002-2024-x, 2002.

497 Emerson, D., and Moyer, C.: Isolation and characterization of novel iron-oxidizing bacteria that

498   grow at circumneutral pH, Appl. Environ. Microb., 63, 4784-4792, 1997.

499 Emerson, D., and Weiss, J. V.: Bacterial iron oxidation in circumneutral freshwater habitats:

500   findings from the field and the laboratory, Geomicrobiol. J., 21, 405-414, 2004.

501   Emerson, D., Weiss, J. V., and Megonigal, J. P.: Iron-oxidizing bacteria are associated with

502   ferric hydroxide precipitates (Fe-plaque) on the roots of wetland plants, Appl. Environ.

503   Microb., 65, 2758-2761, 1999.

504   Emerson, D., Field, E., Chertkov, O., Davenport, K., Goodwin, L., Munk, C., Nolan, M., and

505   Woyke, T.: Comparative genomics of freshwater Fe-oxidizing bacteria: implications for

506   physiology, ecology, and systematics, Front. Microbiol., 4:254,

507   doi:10.3389/fmicb.2013.00254, 2013.

508   Euringer, K., and Lueders, T.: An optimised PCR/T-RFLP fingerprinting approach for the

509   investigation of protistan communities in groundwater environments, J. Microbiol. Meth., 75,

510   262-268, doi:10.1016/j.mimet.2008.06.012, 2008.

511   Fabisch, M., Beulig, F., Akob, D. M., and Küsel, K.: Surprising abundance of *Gallionella*-related

512   iron oxidizers in creek sediments at pH 4.4 or at high heavy metal concentrations, Front.

513   Microbiol., 4:390, doi:10.3389/fmicb.2013.00390, 2013.

514   Fabisch, M., Freyer, G., Johnson, C. A., Büchel, G., Akob, D. M., Neu, T. R., and Küsel, K.:

515   Dominance of '*Gallionella capsiferriformans*' and heavy metal association with *Gallionella*-

516   like stalks in metal-rich pH 6 mine water discharge, Geobiology, submitted, 2015.

517   Fisher, M., Zamir, A., and Pick, U.: Iron uptake by the halotolerant alga *Dunaliella* is mediated

518   by a plasma membrane transferrin, J. Biol. Chem., 273, 17553-17558, 1998.

519   Foster, P. L.: Copper exclusion as a mechanism of heavy metal tolerance in a green alga, Nature,

520   269, 322-323, 1977.

521   Foster, P. L.: Metal resistances of *Chlorophyta* from rivers polluted by heavy metals, Freshwater

522   Biol., 12, 41-61, 1982.

523   Gebühr, C., Pohlon, E., Schmidt, A., and Küsel, K.: Development of microalgae communities in

524   the phytotelmata of allochthonous populations of *Sarracenia purpurea* (Sarraceniaceae),

525   Plant Biol., 8, 849-860, 2006.

526   Geesey, G., Mutch, R., Costerton, J. t., and Green, R.: Sessile bacteria: an important component

527   of the microbial population in small mountain streams, Limnol. Oceanogr., 23, 1214-1223,

528   1978.

529   Greene, B., McPherson, R., and Darnall, D.: Algal sorbents for selective metal ion recovery, in:

530   Metals Speciation, Separation, and Recovery, Lewis Publishers Chelsea, MI, 315-338, 1987.

531   Gudleifsson, B. E.: *Tribonema viride* (*Xanthophyta*) on cultivated grassland during winter and

532   spring, Acta Botanica Islandica, 7, 27-30, 1984.

533   Haack, T. K., and McFeters, G. A.: Microbial dynamics of an epilithic mat community in a high

534   alpine stream, Appl. Environ. Microb., 43, 702-707, 1982.

535   Hallberg, K. B., Coupland, K., Kimura, S., and Johnson, D. B.: Macroscopic streamer growths in

536   acidic, metal-rich mine waters in north wales consist of novel and remarkably simple

537   bacterial communities, Appl. Environ. Microb., 72, 2022-2030, doi:10.1128/aem.72.3.2022-

538   2030.2006, 2006.

539   Hanert, H. H.: The genus *Gallionella*, in: The prokaryotes, Springer Verlag, New York, 990-995,

540   2006.

541   Hedrich, S., Lunsdorf, H., Keeberg, R., Heide, G., Seifert, J., and Schlomann, M.:

542   Schwertmannite formation adjacent to bacterial cells in a mine water treatment plant and in

543   pure cultures of *Ferrovum myxofaciens*, Environ. Sci. Technol., 45, 7685-7692,

544   doi:10.1021/es201564g, 2011a.

545 Hedrich, S., Schlomann, M., and Johnson, D. B.: The iron-oxidizing proteobacteria, Microbiology, 157, 1551-1564, doi:10.1099/mic.0.045344-0, 2011b.

547 Hegler, F., Lösekann-Behrens, T., Hanselmann, K., Behrens, S., and Kappler, A.: Influence of seasonal and geochemical changes on the geomicrobiology of an iron carbonate mineral water spring, Appl. Environ. Microb., 78, 7185-7196, doi:10.1128/aem.01440-12, 2012.

550 Heinzel, E., Janneck, E., Glombitza, F., Schlömann, M., and Seifert, J.: Population dynamics of iron-oxidizing communities in pilot plants for the treatment of acid mine waters, Environ. Sci. Technol., 43, 6138-6144, 2009.

553 Imlay, J. A.: Cellular defenses against superoxide and hydrogen peroxide, Annu. Rev. Biochem., 77, 755-776, doi:10.1146/annurev.biochem.77.061606.161055, 2008.

555 Jiao, Y., Cody, G. D., Harding, A. K., Wilmes, P., Schrenk, M., Wheeler, K. E., Banfield, J. F., and Thelen, M. P.: Characterization of extracellular polymeric substances from acidophilic microbial biofilms, Appl. Environ. Microb., 76, 2916-2922, doi:10.1128/aem.02289-09, 2010.

558 Johnson, C. A., Freyer, G., Fabisch, M., Caraballo, M. A., Küsel, K., and Hochella, M. F.: Observations and assessment of iron oxide and green rust nanoparticles in metal-polluted mine drainage within a steep redox gradient, Environ. Chem., 11, 377-391, doi:10.1071/EN13184, 2014.

562 Johnson, D. B., and Hallberg, K. B.: Carbon, iron and sulfur metabolism in acidophilic micro-organisms, Adv. Microb. Physiol., 54, 201-255, doi:10.1016/s0065-2911(08)00003-9, 2009.

564 Johnsongreen, P. C., and Crowder, A. A.: Iron-oxide deposition on axenic and non-axenic roots of rice seedlings (*Oryza sativa* L.), J. Plant Nutr., 14, 375-386, doi:10.1080/01904169109364209, 1991.

567 Kappler, A., and Straub, K. L.: Geomicrobiological cycling of iron, Rev. Mineral. Geochem., 59,

568   85-108, 2005.

569 Kozubal, M. A., Macur, R. E., Jay, Z. J., Beam, J. P., Malfatti, S. A., Tringe, S. G., Kocar, B. D.,

570   Borch, T., and Inskeep, W. P.: Microbial iron cycling in acidic geothermal springs of

571   Yellowstone National Park: integrating molecular surveys, geochemical processes, and

572   isolation of novel Fe-active microorganisms, Front. Microbiol., 3:109,

573   doi:10.3389/fmicb.2012.00109, 2012.

574 Leduc, L. G., and Ferroni, G. D.: The chemolithotrophic bacterium *Thibacillus ferrooxidans*,

575   FEMS Microbiol. Rev., 14, 103-119, 1994.

576 Levy, J., Stauber, J. L., Wakelin, S. A., and Jolley, D. F.: The effect of bacteria on the sensitivity

577   of microalgae to copper in laboratory bioassays, Chemosphere, 74, 1266-1274,

578   doi:10.1016/j.chemosphere.2008.10.049, 2009.

579 Liu, H., and Buskey, E. J.: Hypersalinity enhances the production of extracellular polymeric

580   substance (EPS) in the Texas brown tide alga, *Aureoumbra lagunensis* (Pelagophyceae), J.

581   Phycol., 36, 71-77, 2000.

582 López-Archilla, A. I., Marin, I., and Amils, R.: Microbial community composition and ecology

583   of an acidic aquatic environment: the Tinto River, Spain, Microb. Ecol., 41, 20-35, 2001.

584 Lüdecke, C., Reiche, M., Eusterhues, K., Nietzsche, S., and Küsel, K.: Acid-tolerant

585   microaerophilic Fe(II)-oxidizing bacteria promote Fe(III)-accumulation in a fen, Environ.

586   Microbiol., 12, 2814-2825, doi:10.1111/j.1462-2920.2010.02251.x, 2010.

587 Machova, K., Elster, J., and Adamec, L.: Xanthophyceaen assemblages during winter-spring

588   flood: autecology and ecophysiology of *Tribonema fonticolum* and *T. monochloron*,

589   Hydrobiologia, 600, 155-168, doi:10.1007/s10750-007-9228-5, 2008.

590   Malik, A.: Metal bioremediation through growing cells, Environ. Int., 30, 261-278, 2004.

591   Neu, T. R., Swerhone, G. D., and Lawrence, J. R.: Assessment of lectin-binding analysis for in

592   situ detection of glycoconjugates in biofilm systems, Microbiology, 147, 299-313, 2001.

593   Neubauer, S. C., Emerson, D., and Megonigal, J. P.: Life at the energetic edge: kinetics of

594   circumneutral iron oxidation by lithotrophic iron-oxidizing bacteria isolated from the

595   wetland-plant   rhizosphere,   Appl.   Environ.   Microb.,   68,   3988-3995,

596   doi:10.1128/aem.68.8.3988-3995.2002, 2002.

597   Peine, A., Tritschler, A., Küsel, K., and Peiffer, S.: Electron flow in an iron-rich acidic sediment

598   - evidence for an acidity-driven iron cycle, Limnol. Oceanogr., 45, 1077-1087, 2000.

599   Picard, A., Kappler, A., Schmid, G., Quaroni, L., and Obst, M.: Experimental diagenesis of

600   organo-mineral structures formed by microaerophilic Fe(II)-oxidizing bacteria, Nature

601   Communications, 6, 6277, doi:10.1038/ncomms7277, 2015.

602   Reed, R., and Gadd, G.: Metal tolerance in eukaryotic and prokaryotic algae, in: Heavy Metal

603   Tolerance in Plants: Evolutionary Aspects, CRC press, Boca Raton, FL, 105-118, 1989.

604   Roth, R. I., Panter, S. S., Zegna, A. I., and Levin, J.: Bacterial endotoxin (lipopolysaccharide)

605   stimulates the rate of iron oxidation, J. Endotoxin Res., 6, 313-319, 2000.

606   Rowe, O. F., Sanchez-Espana, J., Hallberg, K. B., and Johnson, D. B.: Microbial communities

607   and geochemical dynamics in an extremely acidic, metal-rich stream at an abandoned sulfide

608   mine (Huelva, Spain) underpinned by two functional primary production systems, Environ.

609   Microbiol., 9, 1761-1771, doi:10.1111/j.1462-2920.2007.01294.x, 2007.

610   Schädler, S., Burkhardt, C., Hegler, F., Straub, K. L., Miot, J., Benzerara, K., and Kappler, A.:

611   Formation of cell-iron-mineral aggregates by phototrophic and nitrate-reducing anaerobic

Fe(II)-oxidizing bacteria, Geomicrobiol. J., 26:2, 93-103, doi:10.1080/01490450802660573, 2009.

Schloss, P. D., Westcott, S. L., Ryabin, T., Hall, J. R., Hartmann, M., Hollister, E. B., Lesniewski, R. A., Oakley, B. B., Parks, D. H., and Robinson, C. J.: Introducing mothur: open-source, platform-independent, community-supported software for describing and comparing microbial communities, Appl. Environ. Microb., 75, 7537-7541, 2009.

Sengbusch, P. V., and Müller, U.: Distribution of glycoconjugates at algal cell surfaces as monitored by FITC-conjugated lectins. Studies on selected species from *Cyanophyta*, *Pyrrhophyta*, *Raphidophyta*, *Euglenophyta*, *Chromophyta*, and *Chlorophyta*, Protoplasma, 114, 103-113, 1983.

Senko, J. M., Wanjugi, P., Lucas, M., Bruns, M. A., and Burgos, W. D.: Characterization of Fe(II) oxidizing bacterial activities and communities at two acidic Appalachian coalmine drainage-impacted sites, ISME J., 2, 1134-1145, 2008.

Smith, G. M.: Cryptogamic Botany, Vol. 1, Algae and Fungi, McGraw-Hill, New York, 1938.

Steinberg, P. D., Schneider, R., and Kjelleberg, S.: Chemical defenses of seaweeds against microbial colonization, Biodegradation, 8, 211-220, doi:10.1023/a:1008236901790, 1997.

Stevenson, R. J., Bothwell, M. L., Lowe, R. L., and Thorp, J. H.: Algal ecology: Freshwater Benthic Ecosystem, Academic press, San Diego, 1996.

Suzuki, T., Hashimoto, H., Matsumoto, N., Furutani, M., Kunoh, H., and Takada, J.: Nanometer-scale visualization and strucural analysis of the inorganic/organic hybrid structures of *Gallionella ferruginea* twisted stalks, Appl. Environ. Microb., 77, 2877-2881, doi:10.1128/aem.02867-10, 2011.

634   Tabatabai, M. A.: A rapid method for determination of sulfate in water samples, Environ. Lett., 7,

635   237-243, 1974.

636   Tamura, H., Goto, K., Yotsuyan.T, and Nagayama, M.: Spectrophotometric determination of

637   iron(II) with 1,10-phenanthroline in presence of large amounts of iron(III), Talanta, 21, 314-

638   318, doi:10.1016/0039-9140(74)80012-3, 1974.

639   Tang, Y. Z., and Dobbs, F. C.: Green autofluorescence in dinoflagellates, diatoms, and other

640   microalgae and its implications for vital staining and morphological studies, Appl. Environ.

641   Microb., 73, 2306-2313, doi:10.1128/aem.01741-06, 2007.

642   Transeau, E. N.: The periodicity of freshwater algae, Am. J. Bot., 3, 121-133, 1916.

643   Tripathi, R. D., Tripathi, P., Dwivedi, S., Kumar, A., Mishra, A., Chauhan, P. S., Norton, G. J.,

644   and Nautiyal, C. S.: Roles for root iron plaque in sequestration and uptake of heavy metals

645   and metalloids in aquatic and wetland plants, Metallomics, 6, 1789-1800,

646   doi:10.1039/c4mt00111g, 2014.

647   Trouwborst, R. E., Johnston, A., Koch, G., Luther, G. W., and Pierson, B. K.: Biogeochemistry

648   of Fe(II) oxidation in a photosynthetic microbial mat: implications for Precambrian Fe(II)

649   oxidation, Geochim. Cosmochim. Acta, 71:19, 4629-4643, doi:10.1016/j.gca.2007.07.018,

650   2007.

651   Tyson, G. W., Chapman, J., Hugenholtz, P., Allen, E. E., Ram, R. J., Richardson, P. M.,

652   Solovyev, V. V., Rubin, E. M., Rokhsar, D. S., and Banfield, J. F.: Community structure and

653   metabolism through reconstruction of microbial genomes from the environment, Nature, 428,

654   37-43, doi:10.1038/nature02340, 2004.

655   Vinocur, A., and Izaguirre, I.: Freshwater algae (excluding *Cyanophyceae*) from nine lakes and

656   pools of Hope Bay, Antarctic Peninsula, Antarct. Sci., 6, 483-490, 1994.

657   Wang, H., Ji, B., Wang, J., Guo, F., Zhou, W., Gao, L., and Liu, T.: Growth and biochemical

658   composition of filamentous microalgae *Tribonema* sp. as potential biofuel feedstock, Bioproc.

659   Biosyst. Eng., 37, 2607-2613, 2014.

660   Wang, J., Sickinger, M., Ciobota, V., Herrmann, M., Rasch, Helfried, Rösch, P., Popp, J., and

661   Küsel, K.: Revealing the microbial community structure of clogging materials in dewatering

662   wells differing in physico-chemical parameters in an open-cast mining area, Water Res.,

663   63:15, 222-233, doi:10.1016/j.watres.2014.06.021, 2014.

664   Warner, R. W.: Distribution of biota in a stream polluted by acid mine-drainage, Ohio J. Sci., 71,

665   202-215, 1971.

666   Wiegert, R. G., and Mitchell, R.: Ecology of Yellowstone thermal effluent systems: intersects of

667   blue-green algae, grazing flies (*Paracoenia*, Ephydridae) and water mites (*Partnuniella*,

668   Hydrachnellae), Hydrobiologia, 41, 251-271, 1973.

669   Winterbourn, M. J., McDiffett, W. F., and Eppley, S. J.: Aluminium and iron burdens of aquatic

670   biota in New Zealand streams contaminated by acid mine drainage: effects of trophic level,

671   Sci. Total Environ., 254, 45-54, doi:10.1016/s0048-9697(00)00437-x, 2000.

672   Wotton, R. S.: The utiquity and many roles of exopolymers (EPS) in aquatic systems, Sci. Mar.,

673   68, 13-21, 2004.

674   Yu, Q., Matheickal, J. T., Yin, P., and Kaewsarn, P.: Heavy metal uptake capacities of common

675   marine macro algal biomass, Water Res., 33, 1534-1537, 1999.

676

677 **Tables & Figures**

678

679 **Table 1.** Average 16S rRNA gene copy numbers of *Gallionella* detected per gram wet weight

680 algae sampled at sites O, A, B, and C, and at three sampling times in 2013 and measured by

681 quantitative PCR (n=3, $\pm$ SD).

	Site O	Site A	Site B	Site C
July 2013	Not reachable	Green $1.85 \times 10^9 \pm 1.86 \times 10^7$	Green $1.72 \times 10^9 \pm 1.62 \times 10^8$	Brown $0.95 \times 10^9 \pm 6.66 \times 10^7$
August 2013	Green $6.78 \times 10^9 \pm 2.36 \times 10^8$	Green $7.08 \times 10^9 \pm 3.76 \times 10^8$	Brown $1.45 \times 10^9 \pm 1.07 \times 10^8$	Brown $1.25 \times 10^9 \pm 1.62 \times 10^7$
September 2013	Green $2.25 \times 10^9 \pm 1.19 \times 10^7$	Brown $1.10 \times 10^9 \pm 3.47 \times 10^7$	No algae	No algae

682

683
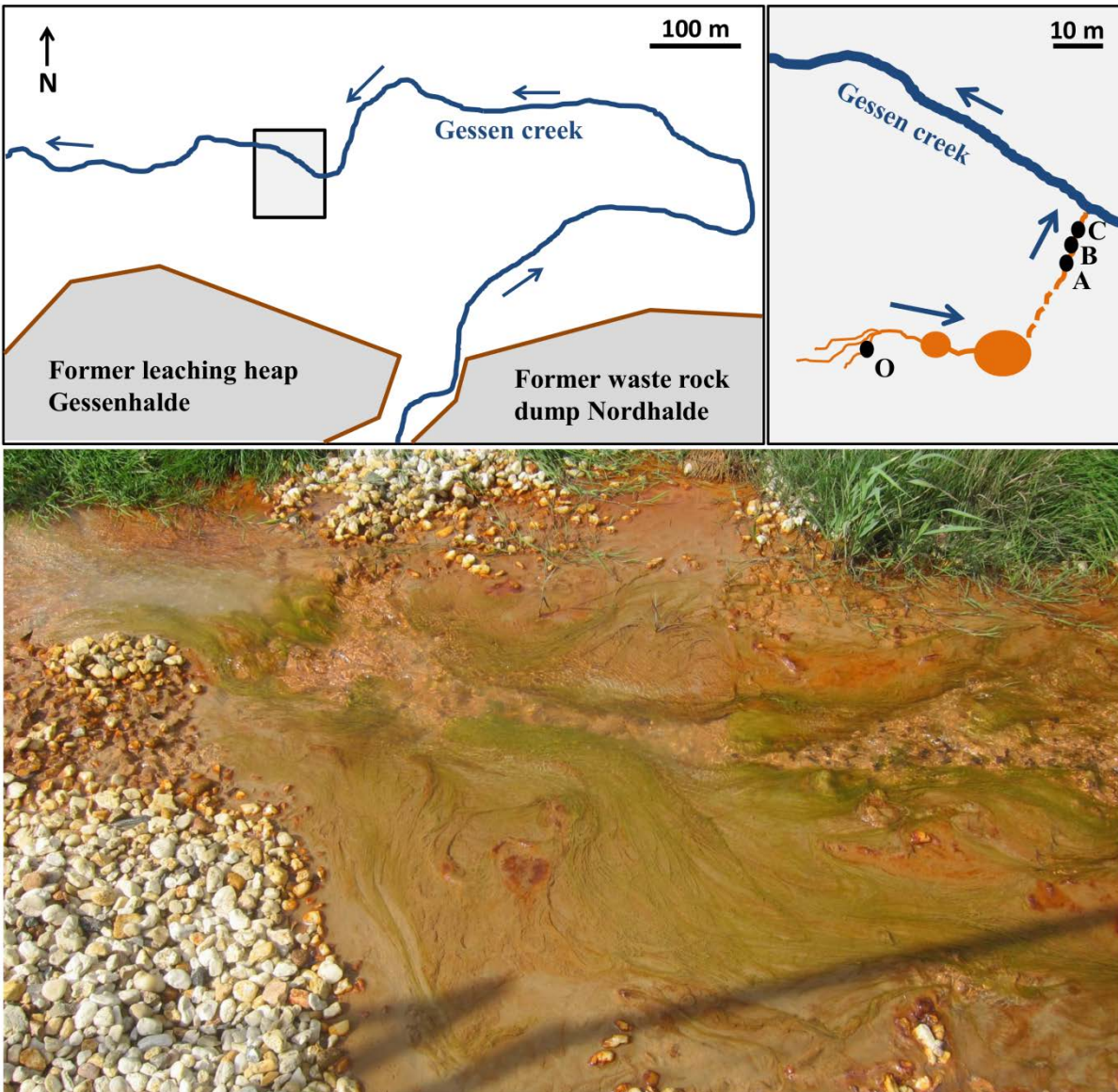
Figure 1. Schematic maps of the study site and photograph of the site A in the former Ronneburg uranium mining district (Thuringia, Germany). Maps show the locations of sampling sites O, A, B and C on the grassland close to Gessen creek. Blue arrows indicate the flow direction of the creek and outflow streams. The photograph was taken in September 2011 and shows the presence of conspicuous green filamentous algae.

689
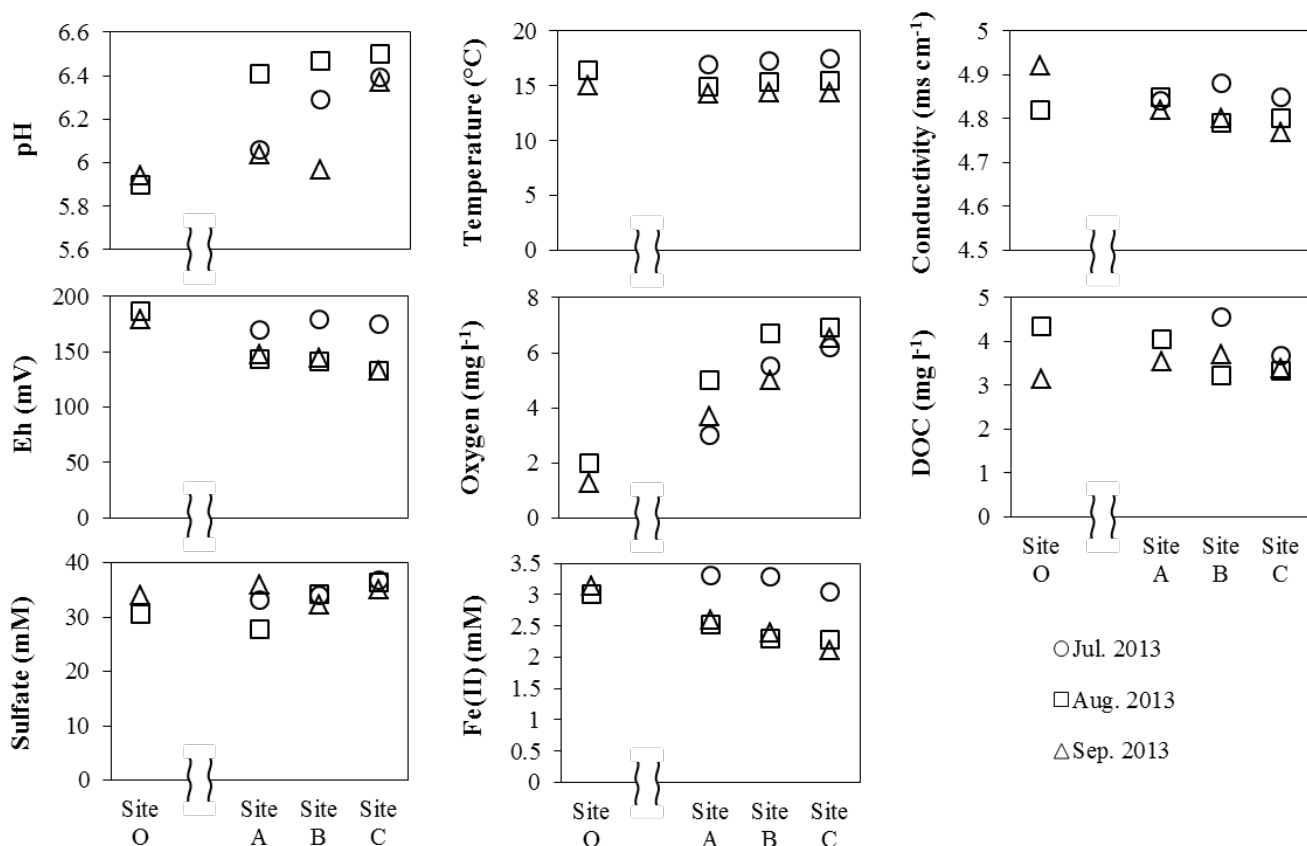
Figure 2. Chemical parameters of water at each sampling site in the outflow water stream. Water pH, oxygen, temperature, conductivity and Eh were measured in the field at site O, A, B and C in July, August, and September 2013. Concentrations of organic carbon, sulfate and Fe(II) were determined later in the laboratory.

694
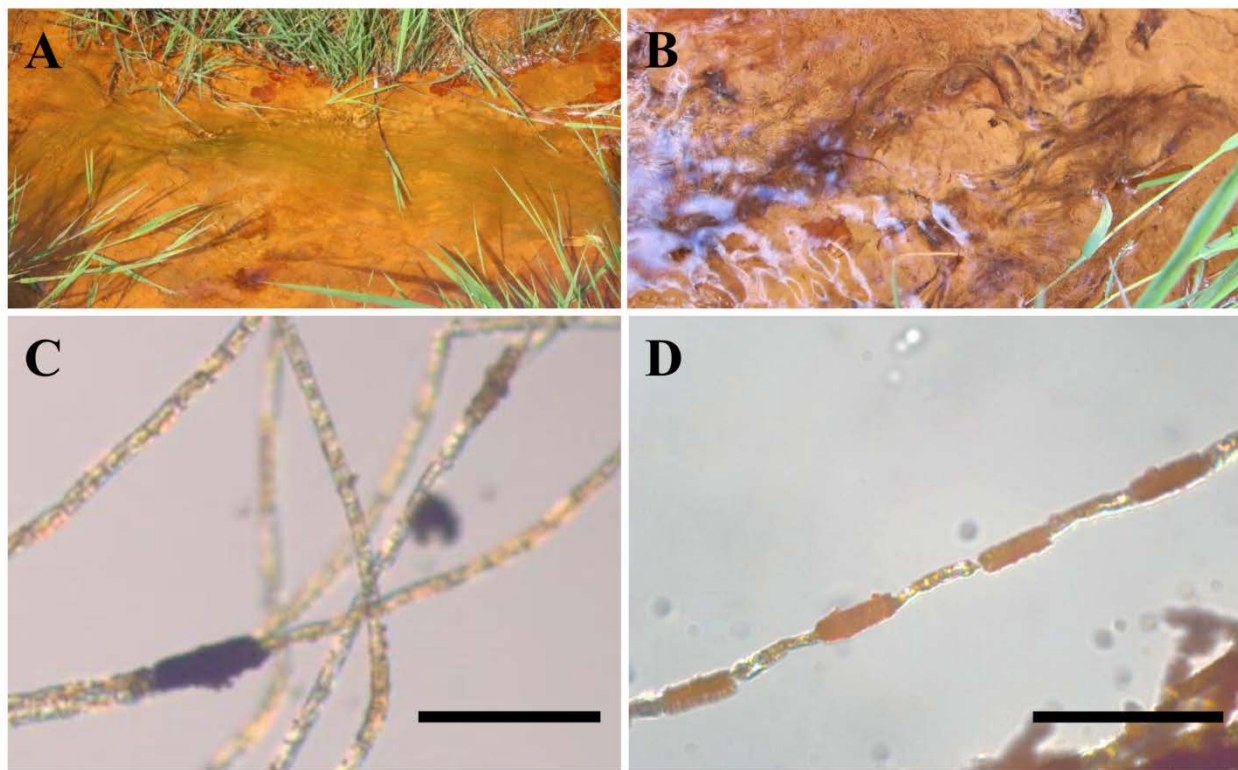
Figure 3. Photographs (A, B) and light microscopic pictures (C, D) of the green algae in site A (A, C) and the brown algae in site C (B, D) taken in July 2013. The microscopic pictures show Fe-mineral precipitates on the algae. Scale bars indicate 100 µm.
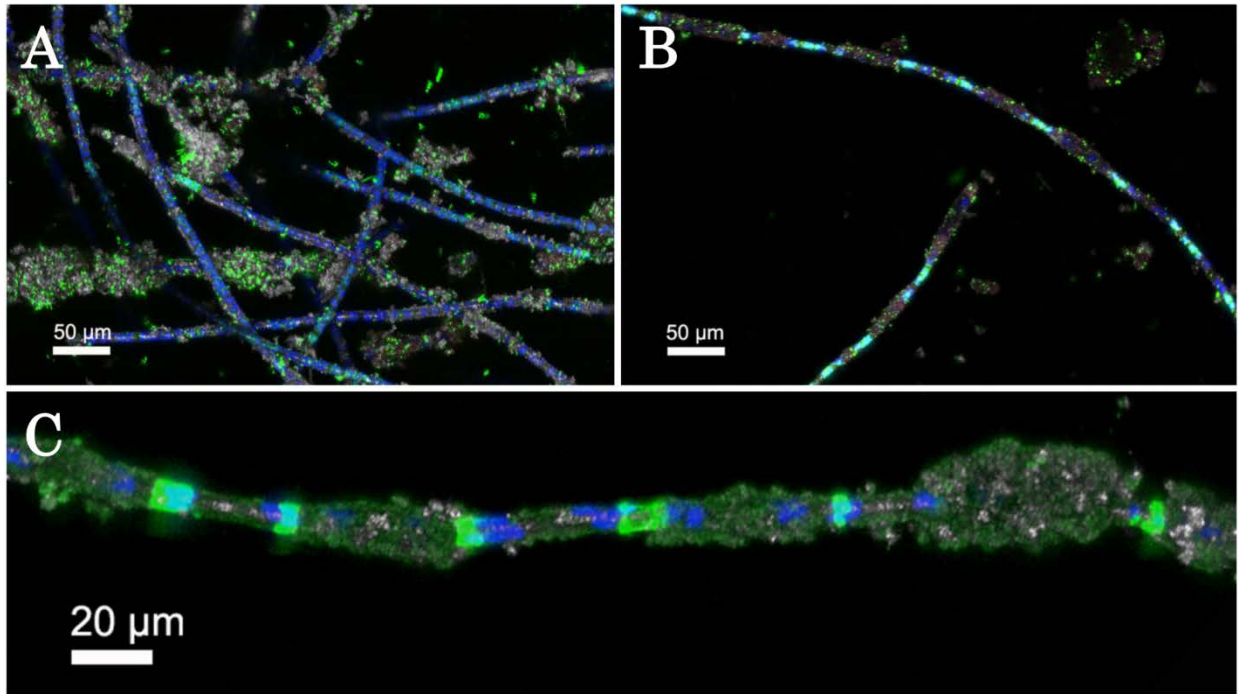
Figure 4. Confocal laser scanning microscopy images of the algae-microbial communities collected at site O (outflow) of the stream in September 2013. Maximum intensity projection of the green algae (A) and the brown algae (B) stained with Syto9 were recorded (color allocation: green – nucleic acid stain; blue – autofluorescence of chlorophyll A; grey - reflection). Brown algae stained with AAL-Alexa448 (C) shows glycoconjugates (green), autofluorescence of chlorophyll A (blue), and refection (grey).

708
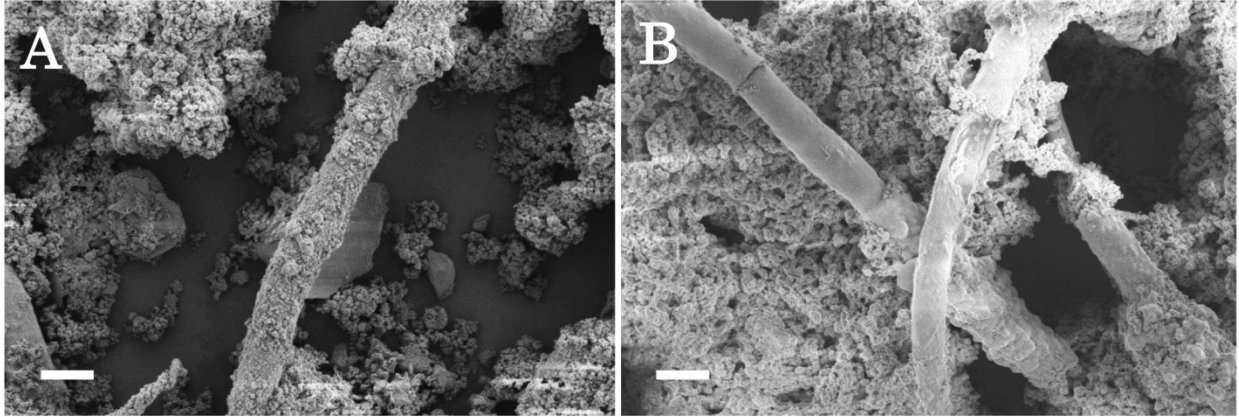
Figure 5. Scanning electron microscopy images of the green algae in site O (A) and the brown

algae in site A (B) taken in September 2013. Scale bars indicate 10 μm.

711
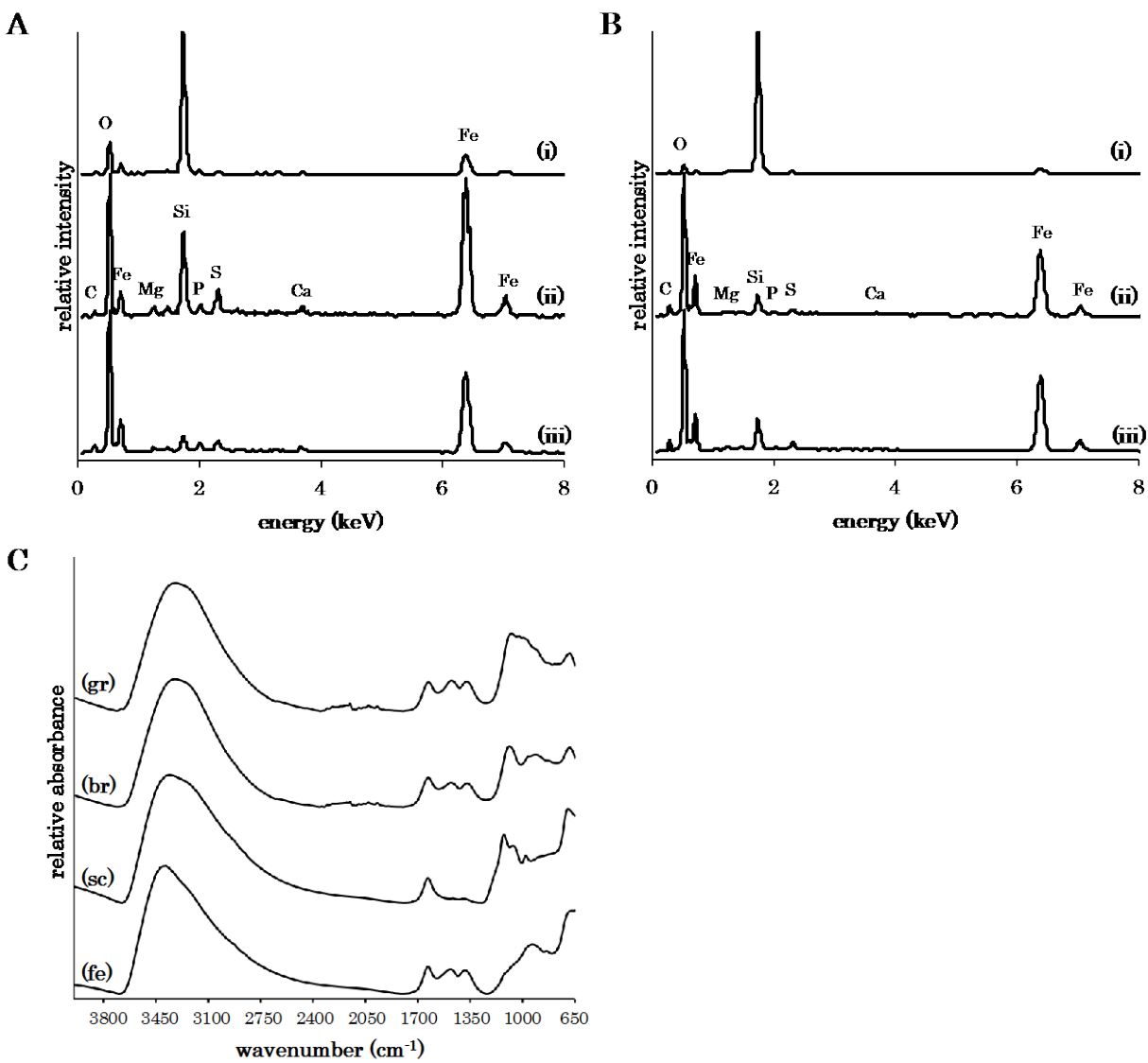
Figure 6. EDX and FTIR spectra of minerals precipitated around the algae. EDX spectra of minerals around the green algae (a) and the brown algae (b) were recorded on the non-encrusted algal surface (i), the encrusted algal surface (ii) and Fe-oxides which were not connected to the algae (iii). FTIR spectra of Fe-oxides (c) were recorded on the green algae (gr) and the brown algae (br), comparing with spectra of schwertmannite (sc) and ferrihydrite (fe) as references.
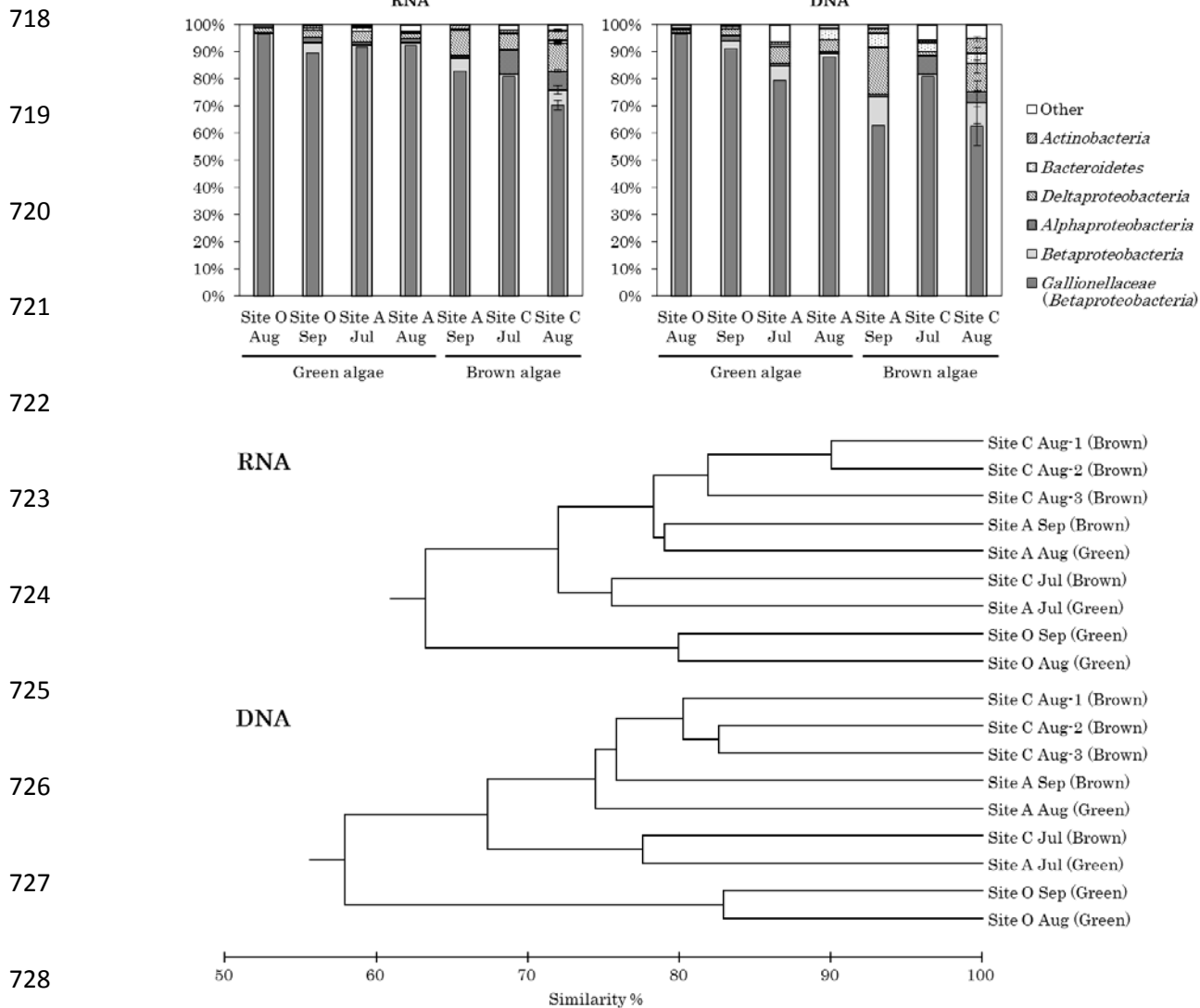
Figure 7. Bacterial community compositions obtained from algal samples detected by 16S rRNA gene-targeted amplicon pyrosequencing (above) and dendrograms indicating similarities of RNA and DNA compositions (below). Calculations of the bacterial populations were based on the total numbers of OTUs associated with phylotypes of sequenced representatives at the phylum level, or class level for Proteobacteria. Percentages of *Gallionellaceae* (*Betaproteobacteria*) were also shown. (n=1; Site C Aug, n=3, error bars indicate SD)